

# UC Davis

## UC Davis Previously Published Works

### Title

Measurement Layout for Residual Stress Mapping Using Slitting

### Permalink

<https://escholarship.org/uc/item/462733nf>

### Journal

Experimental Mechanics, 62(3)

### ISSN

0014-4851

### Authors

Olson, MD  
DeWald, AT  
Hill, MR

### Publication Date

2022-03-01

### DOI

10.1007/s11340-021-00791-w

Peer reviewed

# Measurement layout for residual stress mapping using slitting

M.D. Olson<sup>1</sup>, A.T. DeWald<sup>1</sup>, and M.R. Hill<sup>2</sup>

<sup>1</sup>Hill Engineering, LLC, 3083 Gold Canal Drive, Rancho Cordova, CA

<sup>2</sup>Department of Mechanical and Aerospace Engineering, University of California,

One Shields Avenue, Davis, CA

(Author's accepted manuscript)

Submitted to *Experimental Mechanics*, July 2021

Accepted for publication, September 2021, <https://doi.org/10.1007/s11340-021-00791-w>

---

## ABSTRACT

**Background:** Residual stress spatial mapping has been developed using various measurement methods, one such method comprising a multiplicity of one-dimensional slitting method measurements combined to form a two-dimensional (2D) map. However, an open question is how to best distribute the individual slitting measurements for 2D mapping. **Objective:** This paper investigates the efficacy of different strategies for laying out the individual slitting measurements when mapping in-plane residual stress in thin stainless steel slices removed from a larger dissimilar metal weld. **Methods:** Three different measurement layouts are assessed: independent measurements on nominally identical specimens (i.e., one slitting measurement per specimen, with many specimens), repeatedly bisecting a single slice, and making nominally sequential measurements from one side of the specimen towards the other side of the specimen. Additional comparison measurements are made using neutron diffraction. **Results:** The work shows little difference between the independent and bisecting slitting measurement layouts, and some differences with the sequential measurements. There is good general agreement between neutron diffraction measurement data and the data from the independent and bisecting layouts. **Conclusions:** This work suggests that when using slitting to create a 2D map of in-plane residual stress, a cutting layout that repeatedly bisects the specimen works well, requires a small number of specimens, and avoids potential errors from geometric asymmetry or measurement sequence.

*Keywords:* Residual stress measurement, slitting method, crack compliance method, slitting mapping, biaxial stress mapping, shear stress error

---

## 1. INTRODUCTION

The mapping of residual stresses has been shown to be useful in predicting fatigue life [1,2,3] as well as for prediction of post-machining distortion of parts containing residual stress [4,5]. The only residual stress measurement technique that directly produces a map of residual stress is the contour

\*Corresponding author, Tel: (916) 635-5706, Fax: (916) 604-4517

E-mail address: [molson@hill-engineering.com](mailto:molson@hill-engineering.com)

method [6] and the spatial map of residual stress over the measurement plane has proven useful in a range of applications. The contour method measures the residual stress component normal to the measurement plane. Pagliaro et. al. were the first to combine the contour method with other measurement techniques to determine additional in-plane residual stress components [7].

The current authors have developed an approach that uses slitting to determine a map of one (or more than one) component of the in-plane residual stress [8]. This technique has been deployed on several specimens, including a monolithic airframe structural component [9], a nuclear safety relief valve containing dissimilar metal welds [10], a quenched aluminum bar [11], a machined aluminum T-section, a stainless steel dissimilar metal welded plate, a titanium electron beam welded plate, and a nickel disk forging [12]. Furthermore, the authors have investigated the details of using slitting to form a residual stress map [13]. They found that the minimum distance between slitting measurements was 20% of the specimen thickness (along the direction the slitting measurement will occur). They also conducted a series of numerical experiments to investigate possible errors arising due to shear stress release. They found that when the slitting measurement is close to a free edge and the shear stress at the measurement plane is large, there could be large errors arising from shear stress release, up to 17%.

The aim of the current work is to compare different measurement layouts for slitting mapping. One approach to the measurement layout is to choose the distance between measurements to be large enough that a prior slitting measurement does not affect subsequent measurements as described in [13] and [14]. For that layout, the resulting measurement spacing could be larger than desired. The other extreme of specimen measurement resolution would be to place measurements at 20% of specimen thickness (the limit defined in [13]). A downside of close spacing is that measurement uncertainty increases as spacing decreases [13]. To achieve the aim of this work, residual stress maps are determined using slitting with three different cutting layouts; the layouts employed strike a balance between close and far spacing.

Supplementary neutron diffraction measurements are also made for comparison with results from the three cutting layouts.

## 2. METHODS

### *Specimen description*

The specimens used in this work were taken from a large stainless steel plate that contained a dissimilar metal (DM) weld. The plate was made from 316L stainless steel having a yield strength of 440 MPa. The plate had a 25.4 mm (1.0 in) thickness by 152.4 mm (6.0 in) width cross-section and a length of 1.22 m (48.0 in) (Fig. 1). A slot was machined along the entire length of the plate at the mid-width and was 9.53 mm (0.375 in) deep and 19.05 mm (0.75 in) wide, with a 70° root angle. Prior to filling the slot with weld material, the plate was constrained by welding it to an additional support plate. The weld joining the plate to the support plate was a continuous 7.94 mm (0.313 in) fillet weld that was applied along both 1.22 m edges of the plate. The slot weld was made using eight passes, each continuous along the entire length of the plate, using an automated welder and dissimilar metal (DM) A52M (ERNiCrFe-7A) wire of diameter 0.89 mm (0.035 in). Welding was gas tungsten arc welding (GTAW) with 250 A current, 10.5 V voltage, and 101.6 mm/min (4 in/min) travel speed.

Following welding, the specimens used for this work were prepared. First, the restraining fillet welds were machined away to release the DM welded plate from the support plate. Second, thin slices with thicknesses of 6.35 mm (0.25 in) were removed near the mid-length of the plate. The following material properties were used for the measurements. The elastic modulus used was 203 GPa for the SS 316L plate and 211 GPa for the A52 weld. The Poisson's ratio used was 0.3 for the SS 316L plate and 0.289 for the A52 weld. The coordinate system for the slice has the  $x$ -axis origin at the left hand side of the plate and the  $y$ -axis origin at the bottom of the plate.

### *Slitting measurement description*

A useful summary of the theoretical background for the slitting method of residual stress measurement is given in [15]. The key details are summarized here. The slitting method consists of incrementally cutting the sample along a given measurement plane, here from the top of the plate towards the bottom of the plate (e.g., cutting from  $(x, y_{\max})$  to  $(x, \sim 2 \text{ mm})$ ). After each cut increment, strain was recorded using a bonded strain gage on the back face of the slitting measurement plane ( $x, y \approx 0$ ). The strain versus cut depth data in conjunction with an elastic inverse (e.g., a *compliance matrix*) was used to calculate residual stress on the cut plane.

The slitting method experiments followed the approach described by Hill [16] and Prime [17]. Each measurement used a single strain gage mounted on the bottom of the plate (near  $y = 0$ ) with a 0.813 mm (0.032 in) gage length, and self-temperature compensated for stainless steel. Each slitting measurement consisted of approximately 35 cut depth increments, ranging in size from 0.05 to 1.0 mm. See Fig. 2a for the experimental setup for one of the slitting measurements. A compliance matrix for each slitting measurement was determined using a 2D, plane strain, finite element model and unit pulse basis functions. The model used material properties stated above to match the material properties of the weld and base plate. The compliance matrix model had approximately 300,000 eight-node, biquadratic elements, with 1,000 elements across the width and biased node spacing away from the cut plane, with square elements at the cut plane and element size approximately 10x larger at the free ends. The stress calculation used the procedure described in [18], which employs Tikhonov regularization to minimize the effect of noise in the data. Lastly, since the compliance matrix is computed using a plane strain model, it was scaled using the correction scheme developed by Aydiner and Prime [19] to account for the finite out of plane thickness of the specimen. The uncertainty was computed using a combination of the uncertainty in the calculated residual stress due to the uncertainty in the measured strain data as well

as the uncertainty in the regularization-based smoothing included in the residual stress calculation procedure [20].

The slitting measurements were performed with three different cutting layouts. The first made independent measurements on separate slices (i.e., one slitting measurement per specimen, with many specimens) and will be called the “independent” cutting layout. The independent cutting layout had measurements at nine measurement locations A, C, E, G, I, K, M, O, Q at  $x$  from 35.56 mm to 116.84 mm with increments of 10.16 mm (1.4 in to 4.6 in with increments of 0.4 in) as shown in Fig. 3a. Table 1 lists the measurement locations and the sequence in which the measurements were made.

The second cutting layout will be called the bisecting layout. The bisecting layout has the same locations as the independent layout, but a different sequence such that after the first two measurements the slice was repeatedly bisected (the first two measurements were sufficiently far apart as to be practically independent of one another). The symmetric geometry inherent in the bisecting layout was identified in prior work as being insensitive to error from shear stress on the slitting plane [13]. The measurement locations are shown in Fig. 3a and the sequence of measurements is shown in Table 1 (the sequence being A, Q, I, E, M, C, G, K, O). The positions of the measurement locations are also shown in the Table 1.

The third cutting layout had measurement in sequence from one side of the specimen towards the other side, with space for a second set of sequential measurements to be completed following the first set. Two slices of material (Slice A and Slice B) were used where the measurements in the second slice were offset by 5.08 mm (0.2 in) from those in the first slice. The sequential cutting layout had measurements at locations from  $x = 40.64$  mm to 111.76 mm in increments of 5.08 mm (1.6 in to 4.4 in in increments of 0.2 in). The measurement locations are shown in Fig. 3b and the measurement locations and sequence are listed in Table 1 for Slice A and Slice B.

For the bisecting and sequential layouts, there is a need to correct for the effect of a prior measurement on a subsequent one. For each subsequent measurement, a correction for release of residual stress during the prior measurement is determined following the procedure given in [13] and summarized here. The correction uses the stress determined in the prior measurement as a traction boundary condition input in a supplemental stress analysis whose geometry reflects the configuration of the workpiece prior to the subsequent measurement (i.e., the model uses the geometry following the prior measurement, including cut surfaces created during the prior measurement). The stress measured by the prior measurement is applied as a traction on the prior cut surfaces, and stress is determined at the subsequent measurement plane. The stress at the subsequent measurement plane so determined, gives an estimate of the stress released by the prior measurement and is the correction to be added to the subsequent measurement to correct for the prior stress release.

### 2.1. *Neutron diffraction*

Neutron diffraction measurements were performed to allow a cross method comparison of residual stresses. The measurements were performed at the Neutron Diffraction Stress Mapping Facility (NRSF2) at the High-Flux Isotope Reactor (HFIR) at Oak Ridge National Laboratory. NRSF2 is a monochromatic beam diffractometer. See Fig. 2b for the experimental setup for one of the neutron diffraction measurement points.

The neutron diffraction measurements used standard methodologies [21] and consisted of collecting interatomic lattice spacing data ( $d$ ) in a specimen containing residual stress and lattice spacing data in a stress-free specimen ( $d_0$ ) for three orthogonal directions, and then computing strain and stress [22]. The specimen containing residual stress, used to measure  $d$ , was a separate, but nominally identical slice specimen to those used in the slitting measurements. Measurements in the  $d$  specimen were made along 17 vertical lines at  $x = 35.56$  to  $116.84$  mm with increments of  $5.08$  mm (1.4 to 4.6 in with increments of

0.2 in) (Fig. 4). Lattice spacings were found for the  $311\{hkl\}$  lattice plane and used a gage volume of 2 mm x 2 mm x 2 mm. The stress-free specimens, used to measure  $d_0$ , consisted of a series of five combs that were cut to have cubes with an edge length of 3.0 mm. Four combs had a vertical orientation where there was a transition between the parent material and the weld material. The four vertical combs were centered at  $x = 66.04, 71.12, 76.2, 81.28, \text{ and } 86.36$  mm (2.6, 2.8, 3.0, 3.2, 3.4 in) with the cubes centered at  $y = 2.5, 6, 9.5, 13, 16.5, 20, \text{ and } 23.5$  mm (0.098, 0.236, 0.374, 0.511, 0.650, 0.787, 0.925 in). One comb had a horizontal orientation away from the weld that was centered at  $y = 13$  mm (0.5118 in) with cubes centered at  $x = 35.56, 40.64, 45.72, 50.8, 55.88, 60.96$  mm (1.4, 1.6, 1.8, 2.0, 2.2, 2.4 in). The combs and cuts between cubes were made using wire electric discharge machining (EDM). It was assumed that the chemical composition at each position is identical in the two slices. Each normal component of the residual strain tensor is typically found from the lattice spacing as

$$\varepsilon_i = \frac{d_i - d_{0,i}}{d_{0,i}} \quad (1)$$

where  $\varepsilon_i$  is strain and  $i = x, y, \text{ or } z$ .

The normal components of the residual stress tensor are computed with Hooke's law [12]

$$\sigma_i = \frac{E}{1 + \nu} \left( \varepsilon_i + \frac{\nu}{1 - 2\nu} (\varepsilon_x + \varepsilon_y + \varepsilon_z) \right) \quad (2)$$

for  $i = x, y, \text{ or } z$ , where  $E$  is the elastic modulus and  $\nu$  is Poisson's ratio. Since the present part is a thin plate, the stress state can be assumed to be plane stress ( $\sigma_z = 0$ ). This assumption allows the  $d_0$ -spacing at each measurement point in the intact sample to be calculated as was found in [13] and [23]

$$d_{0,p\sigma} = \frac{1 - \nu}{1 + \nu} d_z + \frac{\nu}{1 + \nu} (d_x + d_y) \quad (3)$$

where  $d_{0,p\sigma}$  is the stress-free lattice spacing using the plane stress assumption. This has the advantage that the lattice spacing is obtained in the intact specimen not in a second specimen. In addition, an

estimate of the normal stresses can then be found using the plane stress assumption and the derived  $d_{0,p\sigma}$  spacing in Eq. (3), namely

$$\sigma_i = \frac{E(d_i - d_z)}{d_z + \nu(d_x + d_y - d_z)} \quad (4)$$

for  $i = x, y$ . The neutron diffraction results below used the plane-stress assumption.

Uncertainty was calculated by propagating the lattice spacing uncertainty through the equations for strain and stress. The material properties used in the stress calculation,  $E_{\{311\}}$  and  $\nu_{\{311\}}$ , were assumed to be the same as the bulk material properties given above.

### 3. RESULTS

The residual stress maps for each of the cutting layouts as well as neutron diffraction are shown in Fig. 5. The results from the different approaches are in general agreement, with low stress away from the weld (under  $\pm 50$  MPa, near  $x = 40$  and  $x = 110$  mm), with high magnitude stress near the weld ( $\approx 125$  MPa, around  $x = 75$  mm). The stresses oscillate along the  $y$ -direction near the weld, with tensile stress at the weld root ( $\approx 125$  MPa near  $y = 18$  mm), compressive stress below the weld root ( $\approx -150$  MPa near  $y = 10$  mm). There are some differences between the different layouts in the weld area, where the independent and bisecting cutting layouts have similar results whereas the sequential cutting layout differs significantly near the weld (up to 100 MPa differences). The ND results show higher magnitude stresses in the weld area, as well as a zone of high magnitude tensile stress ( $\approx 350$  MPa) at the bottom of the plate, opposite the weld, that is not apparent in the slitting results.

The uncertainty for each of the approaches can be seen in Fig. 6. The uncertainty is low magnitude for most of the slitting measurements, where most locations have values below 10 MPa. The uncertainty for the neutron diffraction measurement is nominally constant at 20 MPa.

Line plots comparing the different approaches are shown in Fig. 7 through Fig. 11. The results at the center of the weld at  $x = 76.2$  mm (3.0 in) are shown in Fig. 7. The results show good agreement for the independent and bisecting cutting layouts, except near the bottom of the plate,  $y = 0$  to 5 mm. At the bottom of the plate, the independent and sequential cutting layouts show large magnitude compressive stress (-250 to -150 MPa), whereas the bisecting layout found stress near zero. Fig. 7 shows good agreement between the spatial trends of ND and two of the slitting measurements (independent and bisecting), but the neutron diffraction data appear to be shifted along  $y$  by about +2 mm (to the right in the figure). The measurement using the sequential cutting layout has significantly lower magnitude stress and is in poor agreement with the other measurements.

The results at  $x = 45.72$  mm (1.8 in) are shown in Fig. 8. The results show low magnitude stresses for all the measurements, which is consistent with this position being far from the weld. There is reasonable agreement between the independent and bisecting cutting layouts for  $y < 20$  mm.

The results at  $x = 66.04$  mm (2.6 in), close to the weld toe, are shown in Fig. 9. The results show high magnitude stresses, with good agreement overall among the measurements. There is some deviation between measurements towards the top of the weld and bottom of the plate. The sequential cutting layout measurement does not show compressive stress at the weld crown like the other slitting measurements. The neutron diffraction and sequential cutting layout measurements have much higher magnitude tensile stress towards the bottom of the plate ( $\approx 250$  MPa) than do the independent and bisecting measurements ( $\approx 50$  MPa). Here again we see that the spatial trend in the ND data is shifted in  $y$  by about +2 mm.

The results at  $x = 86.36$  mm (3.4 in), close to the opposite weld toe, are shown in Fig. 10. The results show high magnitude stresses, with good overall agreement among the measurements and similarity to the results at the other weld toe (Fig. 9). There are some deviations between the data from the sequential

layout and the other two layouts toward the top and bottom of the plate, the differences being like those found at the other weld toe. Again, we see a shift in the spatial trend in the ND data.

The results at  $x = 106.68$  mm (4.2 in), far from the weld, are shown in Fig. 11. The results show low magnitude stresses, with nominal agreement among the measurements. These results are similar to those at  $x = 45.72$  mm, also far from the weld.

#### 4. DISCUSSION

The results of ND and slitting measurements are in general agreement, with a few notable differences. As stated earlier, the line plots (Fig. 7 through Fig. 12) show a consistent spatial offset of about 2 mm between the neutron diffraction results and the slitting results. While a spatial positioning error is unexpected given the precision typical of neutron diffraction, shifting the ND data in the plots would greatly improve their agreement with the slitting data.

While there is general agreement between data from all the measurement approaches, there are some notable differences. The most significant differences in the slitting results are where the results for the sequential layout diverge from the other two layouts (independent and bisecting). Slitting data in Fig. 7, at  $x = 76.2$  mm, for example, show a clear departure in results for the sequential layout at all spatial positions. This plane is far from the nearest edge of the part (76.2 mm is 3 times the 25.4 mm part thickness), so the independent layout measurement is expected to be of high quality (the effects of distance from the part boundary are discussed in detail in prior work [13]). This was the third cut in the bisecting layout (see Table 1), where the prior measurements (first and second) were far away (about 1.6 times the part thickness), so the measurement is nearly independent of the prior cuts. However, for the sequential layout, this was the sixth measurement, and the two prior adjacent measurements were close by (10.16 mm, or 0.4 times the thickness). It is possible that the sequence itself affected the results.

To further investigate the potential effect of sequence, an abbreviated sequential cutting layout was used to repeat the measurements near  $x = 76.2$  mm. The repeated measurements were at  $x = 66.04$ ,  $86.36$ , and  $76.2$  mm (2.6, 3.4, 3.0 in), shown in Table 1 as layout “Sequential (v2)”. The results of the repeated measurement at  $x = 76.2$  mm are compared with data from other measurements in Fig. 12. At shallow depths (near  $y = 25$  mm), the new data are similar to those from the prior sequential layout and at deeper depths are largely similar to data from the independent and bisecting layouts. While the new data are somewhat confounding, the data do reinforce the notion of a sequence effect for the sequential layout that is not evident in data from the independent and bisecting layouts, which would be useful to assess in future work.

One plausible cause for the differences between the cutting layouts is an error introduced due to the presence (and release) of shear stresses. Previous research [13] estimated the effects of a relatively large magnitude shear stress on the outcome of a non-symmetric slitting measurement and found in extreme cases that the error could be significant. The earlier work found that the strain due to shear stress is very small relative to that from normal stress, and could be considered negligible when the spacing between measurements is greater than 75% of the specimen thickness. Some measurement spacings in the sequential layout are smaller than 75% of specimen thickness, so that shear stress could have caused systematic error in the sequential measurements. The independent and bisecting layouts are not subject to similar errors from shear stress. The bisecting layout maintains a symmetric sample geometry and strain gage placement, so that shear stress effects cancel out [13]; the independent layout has measurements placed more than 75% of specimen thickness from specimen boundaries.

## 5. CONCLUSIONS

The work here describes the results of three cutting layouts to map in-plane residual stresses using the slitting method in a thin stainless steel slice containing a dissimilar metal weld. The first cutting

layout (independent) made one slitting measurement on each of nine nominally identical specimens. The second cutting layout (bisecting) repeatedly bisected one specimen. The third cutting layout (sequential) made measurements sequentially from one side of the specimen towards the other side, with one set of measurements following a first set. Results from the independent and bisecting layouts were found to be in good agreement, while results from the sequential layout exhibited notable differences. The data from slitting mapping measurements were compared with data from neutron diffraction measurements, which were in reasonable agreement with the slitting data for independent and bisecting layouts. In summary, the bisecting cutting layout was shown to be a good choice for slitting mapping since it uses a small number of specimens while providing data similar to those obtained from a set of independent measurements requiring multiple coupons.

#### **ETHICAL STATEMENT/CONFLICT OF INTEREST**

The authors have no conflicts of interest to disclose and did not involve human or animal participants nor was informed consent applicable.

#### **ACKNOWLEDGEMENTS**

A portion of this research was performed at ORNL's High-Flux Isotope Reactor and sponsored by the Scientific User Facilities Division, Office of Basic Energy Sciences, US Department of Energy. The authors acknowledge the help of two Electric Power Research Institute programs in provisioning the plate used in this study, with funding from the Materials Reliability Program (Paul Crooker, Principal Technical Leader) and design and fabrication support from the Welding Research and Technology Center.

#### **REFERENCES**

- [1] Stuart, D. H. (2010). Evaluation of Linear Elastic Fracture Mechanics Predictions of One and Two-Dimensional Fatigue Crack Growth at Cold-Expanded Holes [University of California, Davis]. All

Papers/S/Stuart 2010 - Evaluation of Linear Elastic Fracture Mechanics Predictions of One and Two-Dimensional Fatigue Crack Growth at Cold-Expanded Holes.pdf

- [2] Cuellar, S. D., Hill, M. R., DeWald, A. T., & Rankin, J. E. (2012). Residual stress and fatigue life in laser shock peened open hole samples. *Int. J. Fatigue*, 44, 8–13. All Papers/C/Cuellar et al. 2012 - Residual stress and fatigue life in laser shock peened open hole samples.pdf
- [3] Webster, G. A., & Ezeilo, A. N. (2001). Residual stress distributions and their influence on fatigue lifetimes. *Int. J. Fatigue*, 23, Supple, 375–383. [https://doi.org/10.1016/S0142-1123\(01\)00133-5](https://doi.org/10.1016/S0142-1123(01)00133-5)
- [4] Yaghi, A., Ayvar-Soberanis, S., Moturu, S., Bilkhu, R., & Afazov, S. (2019). Design against distortion for additive manufacturing. *Additive Manufacturing*, 27, 224–235. <https://doi.org/10.1016/j.addma.2019.03.010>
- [5] Li, J.-G., & Wang, S.-Q. (2016). Distortion caused by residual stresses in machining aeronautical aluminum alloy parts: recent advances. *The International Journal of Advanced Manufacturing Technology*, 89, 997–1012. <https://doi.org/10.1007/s00170-016-9066-6>
- [6] Prime, M. B. (2010). *The Contour Method: Capabilities, Limitations, and Recent Advances*. All Papers/P/Prime 2010 - The Contour Method - Capabilities, Limitations, and Recent Advances.pdf
- [7] Pagliaro, P., Prime, M. B., Robinson, J. S., Clausen, B., Swenson, H., Steinzig, M., & Zuccarello, B. (2011). Measuring Inaccessible Residual Stresses Using Multiple Methods and Superposition. *Experimental Mechanics*, 51(7), 1123–1134. <https://doi.org/10.1007/s11340-010-9424-5>
- [8] Olson, M. D., & Hill, M. R. (2015). A New Mechanical Method for Biaxial Residual Stress Mapping. *Exp. Mech.*, 55(6), 1139–1150.
- [9] Olson, M. D., Spradlin, T. J., DeWald, A. T., & Hill, M. R. (2018). Multi-Technique Residual Stress Measurements to Quantify Stress Relief of 7085-T7452 Aluminum Die Forgings. *Materials Performance and Characterization*, 7(4).
- [10] Hill, M. R., Olson, M. D., & DeWald, A. T. (2016). Biaxial Residual Stress Mapping for a Dissimilar Metal Welded Nozzle. *J. Pressure Vessel Technol.*, 138(1), 11404. <https://doi.org/10.1115/1.4031504>
- [11] Olson, M. D., Robinson, J. S., Wimpory, R. C., & Hill, M. R. (2016). Characteriation of residual stresses in heat treated, high strength aluminium alloy extrusions. *Mater. Sci. Technol.*, 0(0), 1–12. <https://doi.org/10.1080/02670836.2016.1164973>
- [12] Olson, M. D., DeWald, A. T., & Hill, M. R. (2018). Assessment of Primary Slice Release Residual Stress Mapping in a Range of Specimen Types. *Exp. Mech.* <https://doi.org/10.1007/s11340-018-0420-5>
- [13] Olson, M. D., & Hill, M. R. Two-Dimensional Mapping of In-plane Residual Stress with Slitting. *Exp. Mech.*, 58(1), 151–166, 2018, <https://doi.org/10.1007/s11340-017-0330-y>
- [14] Salehi, S. D. and Shokrieh, M. M., Repeated slitting safe distance in the measurement of residual stresses, *International Journal of Mechanical Sciences*, vol. 157, pp. 599-608, Jul. 2019, <https://doi.org/10.1016/j.ijmecsci.2019.05.010>
- [15] Schajer, G. S. and Prime, M. B., “Use of Inverse Solutions for Residual Stress Measurements,” *J. Eng. Mater. Technol.*, vol. 128, no. 3, pp. 375–382, Jul. 2006.

- [16] Hill, M.R., "The Slitting Method," in Practical Residual Stress Measurement Methods, G. S. Schajer, Ed. West Sussex, UK: John Wiley & Sons, 2013, pp. 89–108.
- [17] M. B. Prime, "Experimental Procedure for Crack Compliance (Slitting) Measurements of Residual Stress," Los Alamos National Laboratory Report (LA-UR-03-8629), 2003.
- [18] G. S. Schajer and M. B. Prime, "Use of Inverse Solutions for Residual Stress Measurements", *Journal of Engineering Materials and Technology*, vol. 128, p. 375, 2006.
- [19] C. Aydiner, and M. B. Prime, Three-Dimensional Constraint Effects on the Slitting Method for Measuring Residual Stress. *J. Eng. Mater. Technol.*, 135(3), 31006, 2013.  
<https://doi.org/10.1115/1.4023849>
- [20] M. D. Olson, A. T. Dewald, and M. R. Hill, An Uncertainty Estimator for Slitting Method Residual Stress Measurements Including the Influence of Regularization, *Exp. Mech.*, 2019.
- [21] ISO, "Non-destructive testing - Standard test method for determining residual stresses by neutron diffraction," International Organization for Standardization, ISO/TS 21432, 2005.
- [22] H. W. Coleman and W. G. Steele, in *Experimentation, Validation, and Uncertainty Analysis for Engineers*, 3rd ed., Hoboken, New Jersey: John Wiley & Sons, Inc., 2009.
- [23] Olson, M. D., Hill, M. R., Clausen, B., Steinzig, M., & Holden, T. M., Residual Stress Measurements in Dissimilar Weld Metal. *Experimental Mechanics*, 55(6), 1093–1103.  
<https://doi.org/10.1007/s11340-015-0010-8>, 2015

## TABLES

<b>Location Code</b>	<b>A</b>	<b>B</b>	<b>C</b>	<b>D</b>	<b>E</b>	<b>F</b>	<b>G</b>	<b>H</b>	<b>I</b>	<b>J</b>	<b>K</b>	<b>L</b>	<b>M</b>	<b>N</b>	<b>O</b>	<b>P</b>	<b>Q</b>
x (mm)	35.6	40.6	45.7	50.8	55.9	61.0	66.0	71.1	76.2	81.3	86.4	91.4	96.5	101.6	106.7	111.8	116.8
x (inch)	1.40	1.60	1.80	2.00	2.20	2.40	2.60	2.80	3.00	3.20	3.40	3.60	3.80	4.00	4.20	4.40	4.60
<b>Cutting Layout</b>	<b>Measurement Sequence</b>																
Independent	1		1		1		1		1		1		1		1		1
Bisecting	1		6		4		7		3		8		5		9		2
Sequential A			1		5		2		6		3		7		4		
Sequential B		1		5		2		6		3		7		4		8	
Sequential "v2"							1		3		2						

*Table 1: Measurement locations and sequences*

## FIGURES



*Fig. 1 – Photo of the full stainless steel dissimilar metal welded plate that the slices were removed from. The plate has global dimensions of approximately 1220 mm x 152 mm x 25.4 mm (48 in x 6 in x 1 in) (excluding weld bead). Slices were removed near the mid-length of the plate and have a thickness of 6.35 mm (0.25 in)*

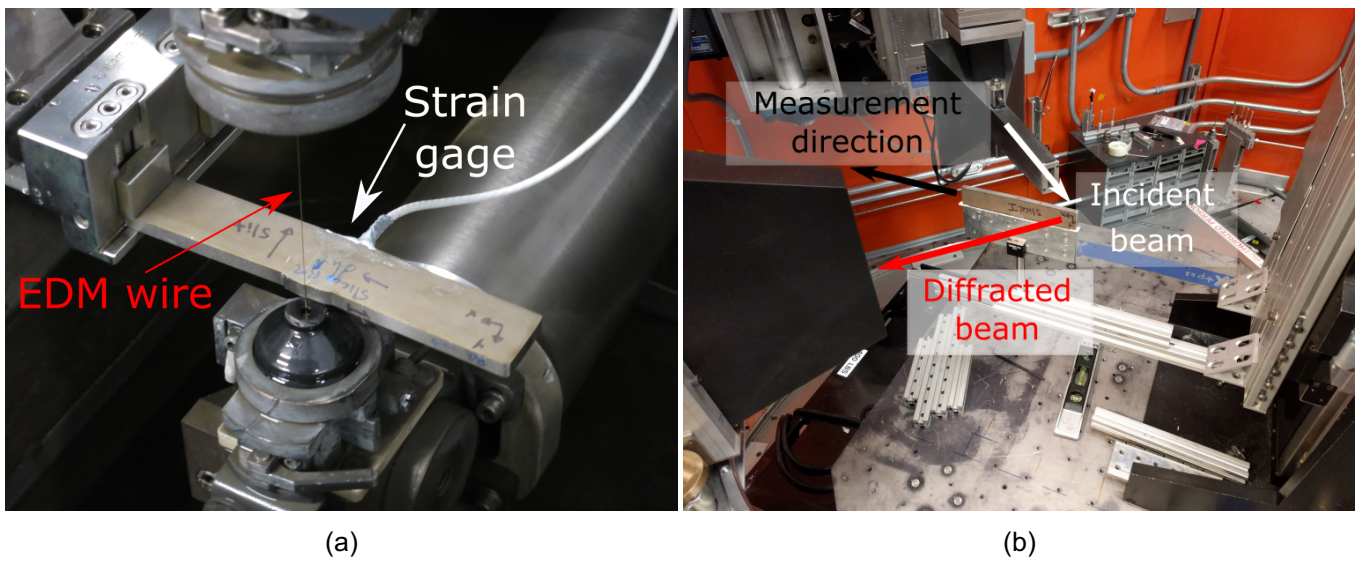


*Fig. 2 – Experimental setup for (a) one of the slitting measurements and (b) neutron diffraction measurement points.*

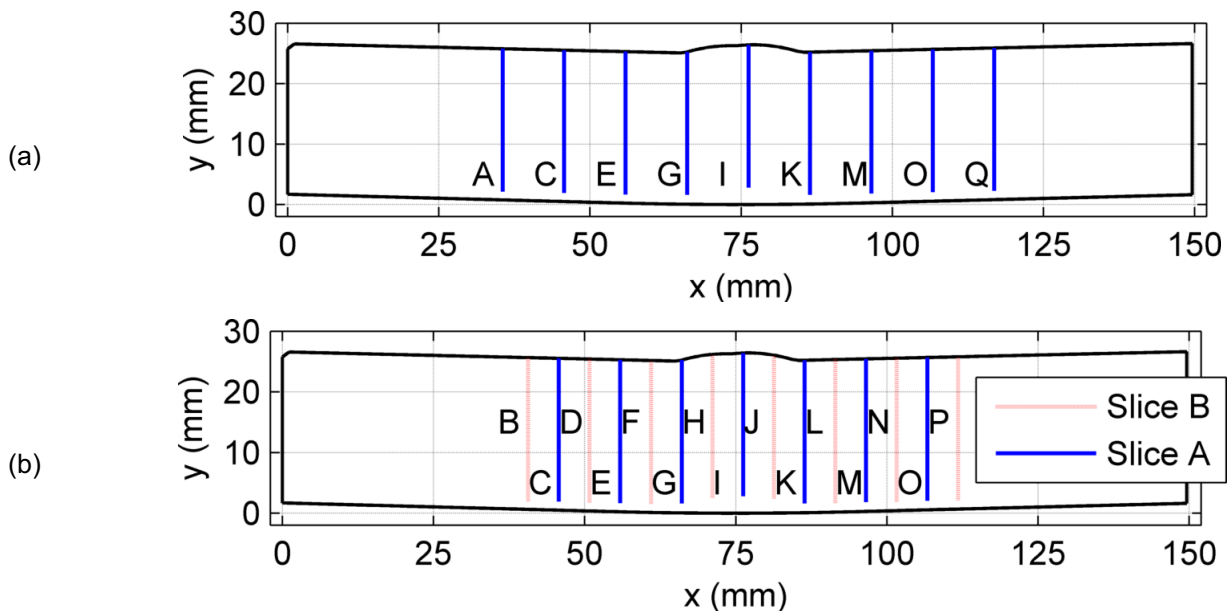


Fig. 3 – Slitting measurement locations for the (a) “independent” (9 specimens) and “bisecting” (1 specimen) cutting order layouts and (b) “sequential” (2 specimens) cutting order layout. The cutting order for the “bisecting” cutting order is A, Q, I, E, M, C, G, K, O. The cutting order for the “sequential” cutting order is C, G, K, O, E, I, M for Slice A and B, F, J, N, D, H, L, P for Slice B

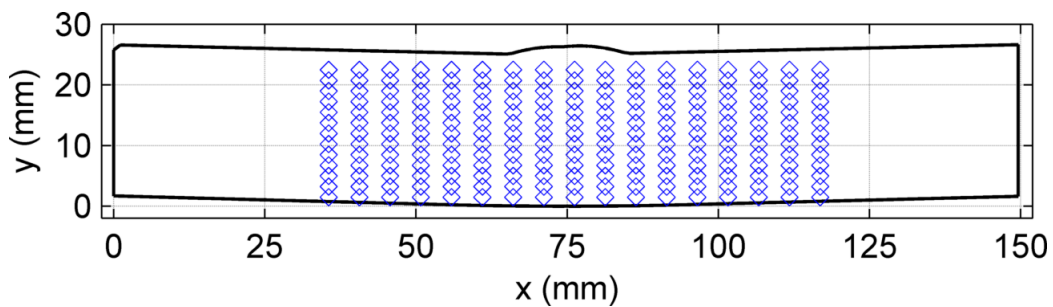
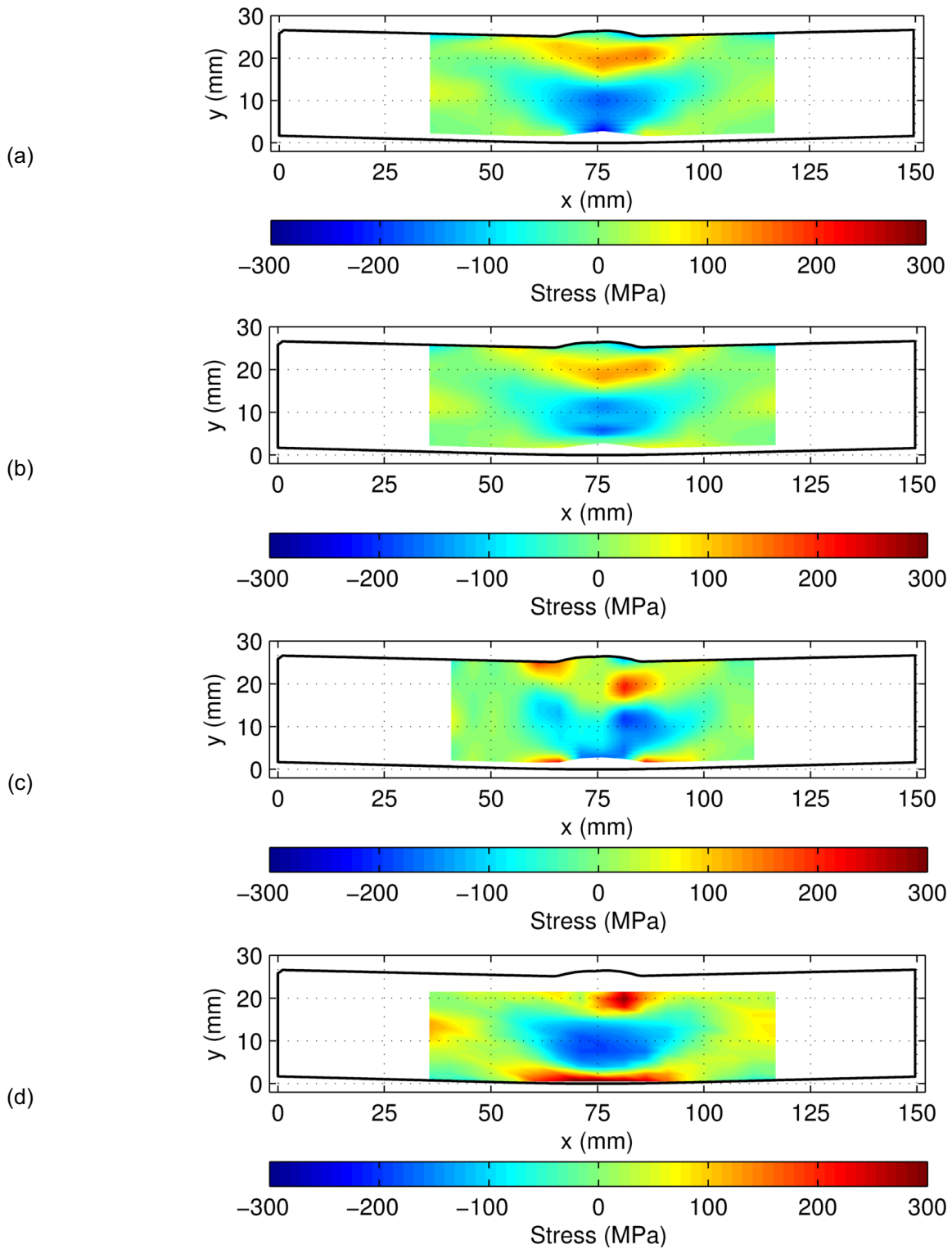


Fig. 4 – Neutron diffraction measurement locations



*Fig. 5 – Stress maps for the (a) independent (b) bisecting, (c) sequential cutting order layouts, and (d) neutron diffraction*

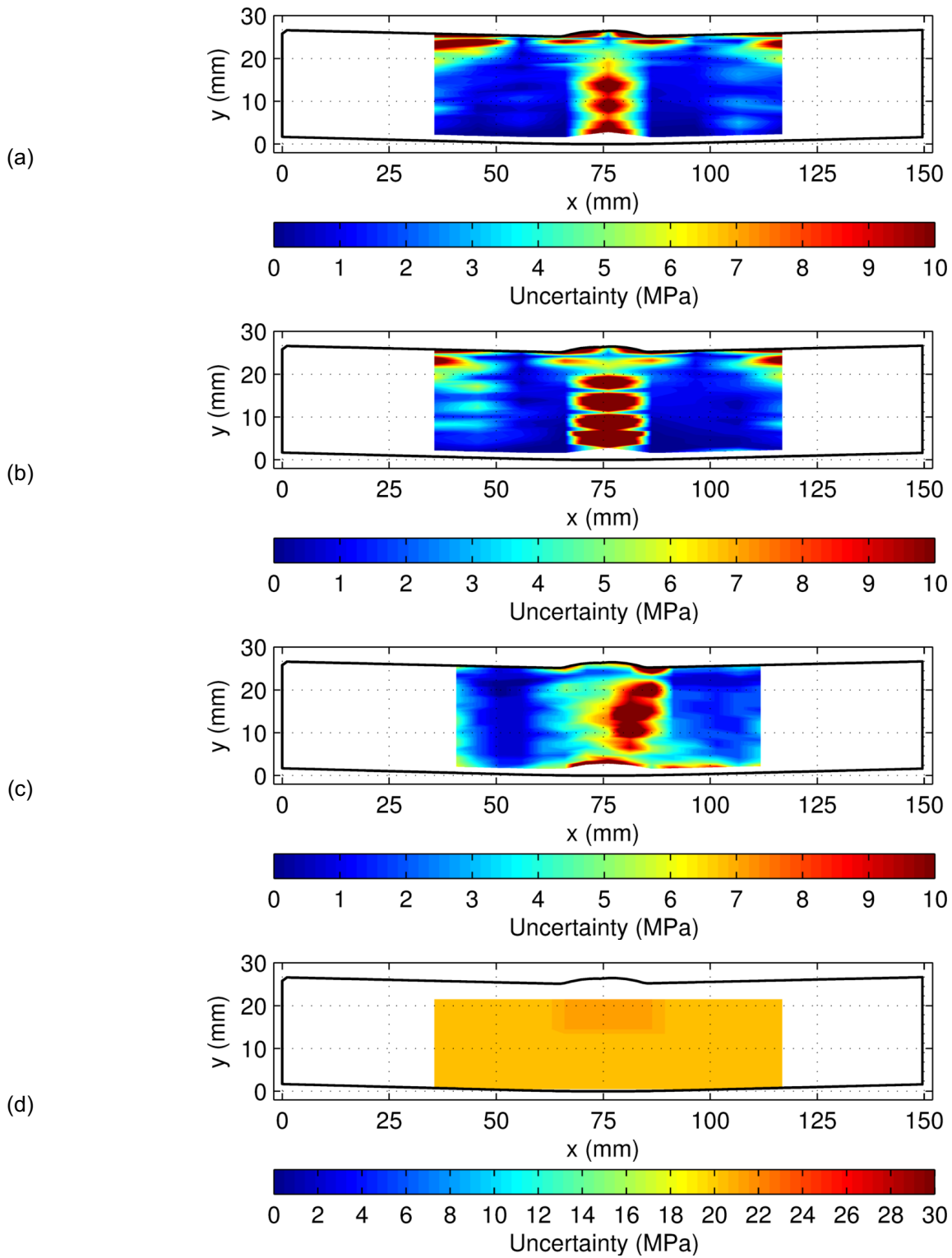


Fig. 6 – Uncertainty for the (a) independent (b) bisecting, (c) sequential cutting order layouts, and (d) neutron diffraction. Note: the neutron diffraction color range (0-30 MPa) is different from the slitting color range (0-10 MPa)

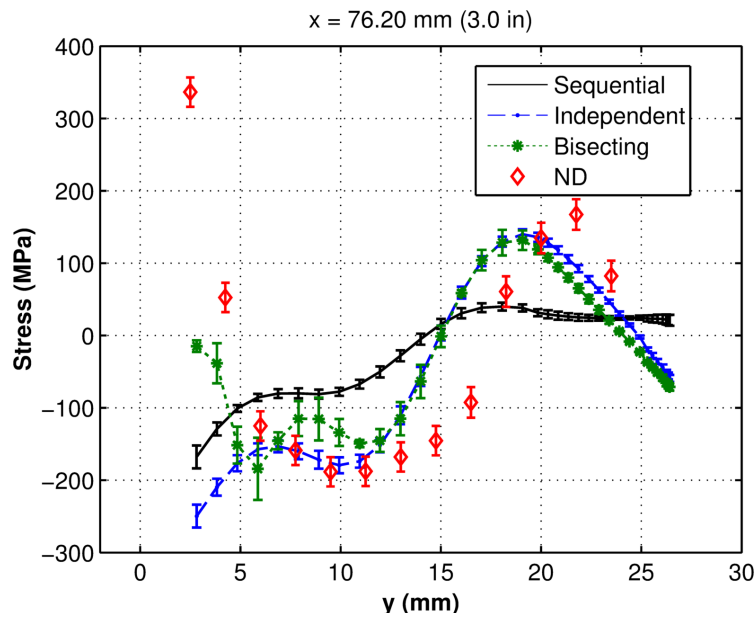


Fig. 7 – Line plot comparing the results from the different measurement approach at the weld center,  $x = 76.2 \text{ mm}$

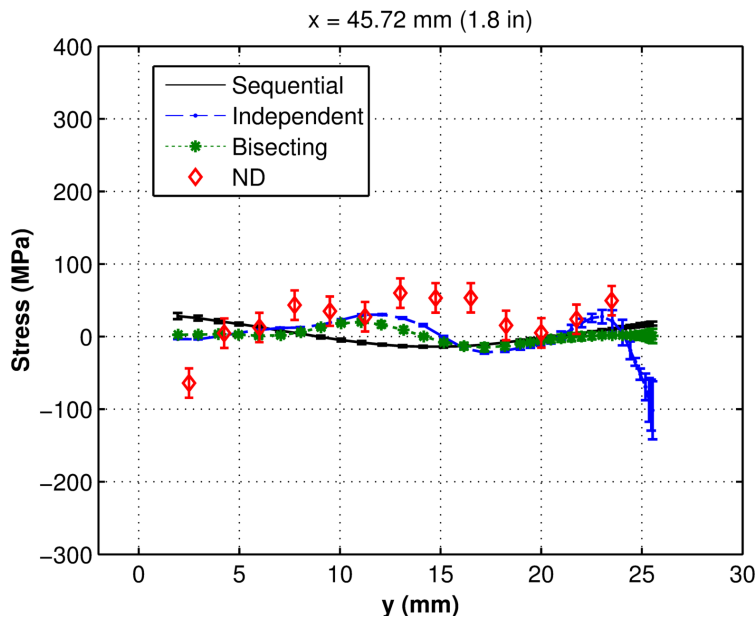


Fig. 8 – Line plot comparing the results from the different measurement approach at  $x = 45.72 \text{ mm}$

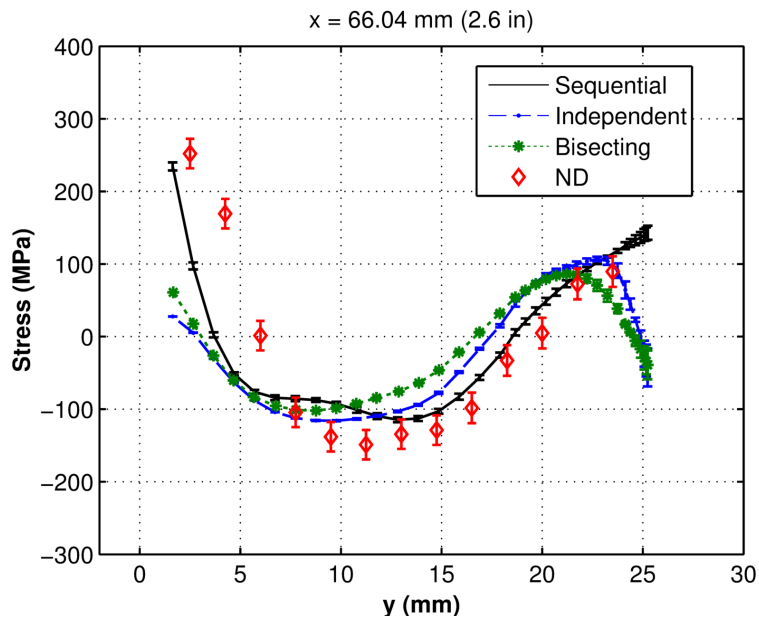


Fig. 9 – Line plot comparing the results from the different measurement approach at x = 66.04 mm

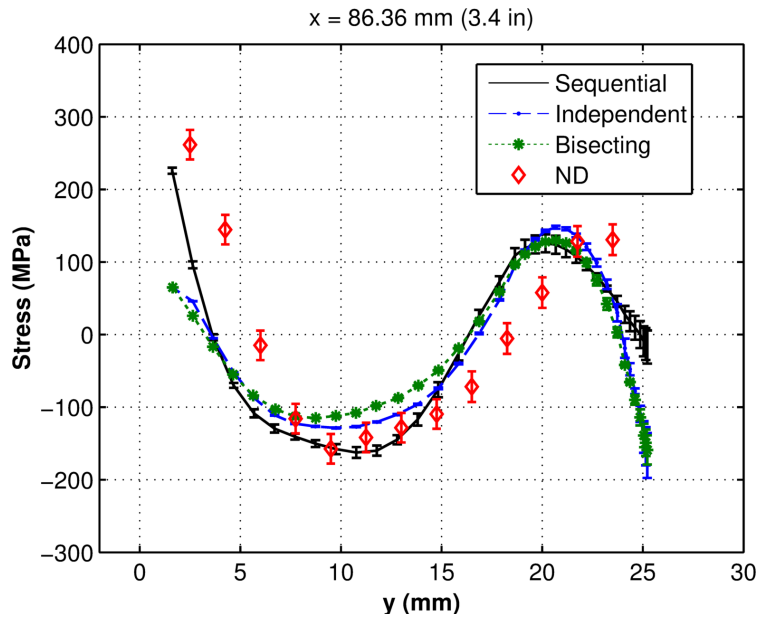


Fig. 10 – Line plot comparing the results from the different measurement approach at x = 86.36 mm

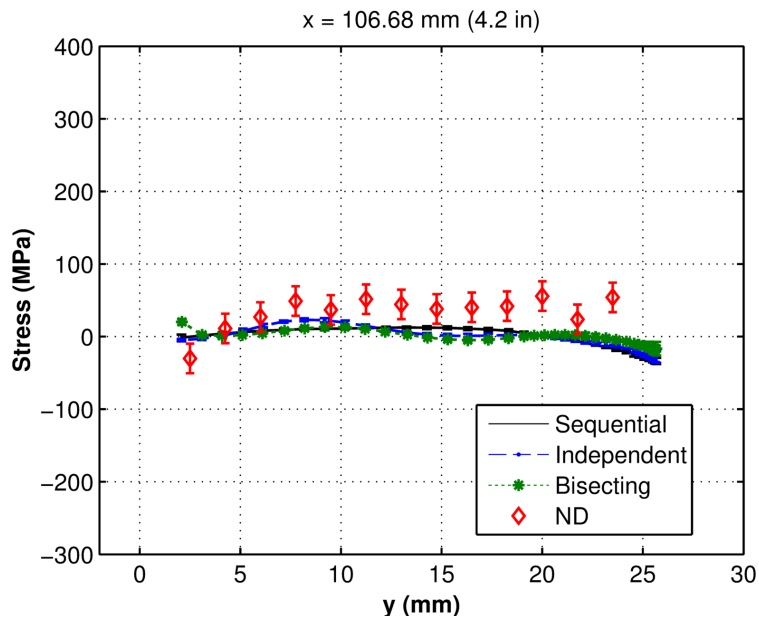


Fig. 11 – Line plot comparing the results from the different measurement approach at  $x = 106.68 \text{ mm}$

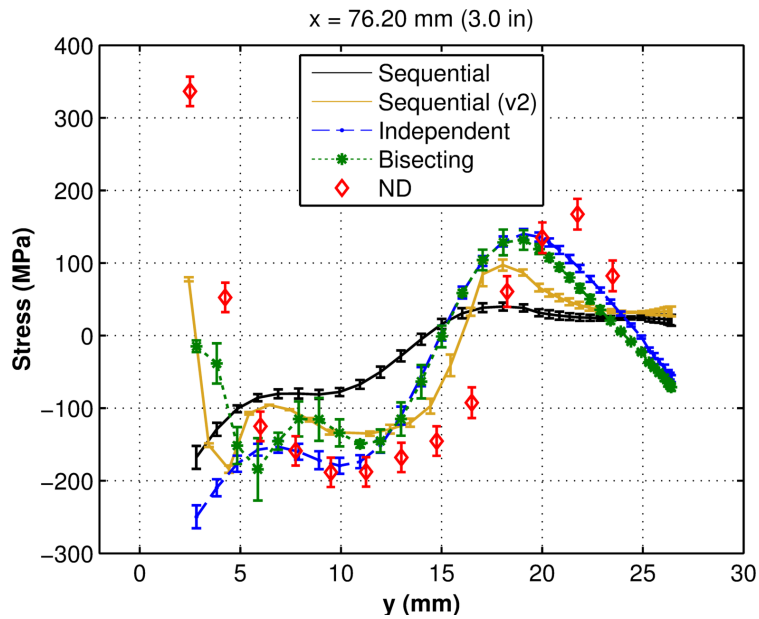


Fig. 12 – Line plot comparing the results from the different measurement approach at  $x = 76.2 \text{ mm}$ , where “Sequential (v2)” is a repeat of the slitting measurement using the same approach as the original sequential cutting layouts